ISSN 1070-3284, Russian Journal of Coordination Chemistry, 2019, Vol. 45, No. 12, pp. 856–866. © Pleiades Publishing, Ltd., 2019.
Russian Text © The Author(s), 2019, published in Koordinatsionnaya Khimiya, 2019, Vol. 45, No. 12, pp. 734–745.

Cyclometalated Iridium(III) Complexes with a Norbornene-Substituted Picolinate Ligand and Electroluminescent Polymers Based on Them

Yu. E. Begantsova[a], L. N. Bochkarev[a], *, E. V. Baranov[a], and V. A. Ilichev[a]

[a] *G.A. Razuvaev Institute of Organometallic Chemistry, Russian Academy of Sciences, Nizhny Novgorod, 603950 Russia*

**e-mail: lnb@iomc.ras.ru*

Received April 16, 2019; revised July 3, 2019; accepted July 8, 2019

Abstract—New cyclometalated iridium(III) complexes, NBEpicIr(Ppy)$_2$ (**I**) and NBEpicIr(Dfppy)$_2$ (**II**), were synthesized (NBEpicH = 3-(((1*S*,4*S*)-bicyclo[2.2.1]hept-5-ene-2-carbonyl)oxy)picolinic acid, PpyH = 2-phenylpyridine, DfppyH = 2-(2,4-difluorophenyl)pyridine). Complex **I** was characterized by X-ray diffraction analysis (CIF file CCDC no. 1878882). Ring opening metathesis polymerization involving compounds **I** and **II** and carbazole norbornene monomers gave new iridium-containing copolymers. The photophysical properties of complexes **I** and **II** and copolymers based on them were studied.

Keywords: cyclometalated iridium complexes, iridium-containing polymers, metathesis polymerization, photoluminescence, electroluminescence

DOI: 10.1134/S1070328419120029

INTRODUCTION

Homo- and heteroligand cyclometalated iridium(III) complexes attract considerable interest owing to their unique photophysical properties and a broad range of applications [1–6]. A major trend is their use as emitters for organic light emitting diodes (OLEDs) [1, 3, 4]. The emitter efficiency and the emission color largely depend on the nature of ligands attached to iridium [1–3]. Apart from low-molecular-weight luminophoric iridium complexes, a large number of iridium-containing polymeric emitters have also been now synthesized [2, 7]. Among the electroluminescent iridium-containing polymers, blue emitters are least studied and least efficient [7]. Therefore, the preparation of new iridium-containing polymers useful as blue electroluminescent materials appears to be an important and relevant task.

It is known that inclusion of a picolinate ligand into cyclometalated iridium complexes induces a blue shift of the emission band in the photoluminescence (PL) and electroluminescence (EL) spectra of iridium luminophores [2, 8]. A similar effect is observed for polymeric emitters containing iridium complexes with picolinate ligands [7]. Apart from the use in light emitting diodes, these iridium-containing polymers were employed to design memory devices and luminescent markers for biological objects [9, 10].

This communication reports the synthesis of two new bis-cyclometalated iridium(III) complexes, NBEpicIr(Ppy)$_2$ (**I**) and NBEpicIr(Dfppy)$_2$ (**II**) (NBEpicH = 3-(((1*S*,4*S*)-bicyclo[2.2.1]hept-5-ene-2-carbonyl)oxy)picolinic acid, PpyH = 2-phenylpyridine, DfppyH = 2-(2,4-difluorophenyl)pyridine), and their ring-opening metathesis polymerization (ROMP) to give polymers P1–P4, which exhibit green and blue-green PL and EL.

EXPERIMENTAL

All operations with easily oxidizable and hydrolyzable compounds were carried out in vacuum or in argon using the standard Schelnk technique. The solvents were thoroughly dried and degassed.

The compounds PpyH, DfppyH, 3-hydroxypicolinic acid (HOpicH), 4,7-diphenyl-1,10-phenanthroline (BATH), and tris(8-hydroxyquinolinato)aluminum (Alq_3) (Aldrich) were used as received. The cyclometalated dimeric chlorides $[(L)_2Ir(\mu\text{-}Cl)]_2$ and the complexes $(L)_2Ir(HOpic)$ (L = Ppy, Dfppy) were synthesized as described in [11, 12]. Carbazole monomers, 9-(bicyclo[2.2.1]hept-5-en-2-ylmethyl)-9H-carbazole (**L^1**) [13] and bicyclo[2.2.1]hept-5-en-2-yl(9H-carbazol-9-yl)methanone (L^2) [14], and $(H_2IMes)(3\text{-}Br\text{-}Py)_2(Cl)_2Ru{=}CHPh$ (third-generation Grubbs catalyst) [15], were prepared by known procedures.

^{1}H and ^{13}C{1H} NMR spectra were recorded on Bruker DPX-200 (^{1}H NMR: 200 MHz; ^{13}C NMR: 50 MHz) and Bruker Avance III-400 (^{1}H NMR: 400 MHz; ^{13}C NMR: 100 MHz) instruments. The

chemical shifts are given in ppm and referenced to internal tetramethylsilane.

IR spectra were measured on an FSM 1201 Fourier transform IR spectrometer. The samples of compounds **I** and **II** were prepared as mineral oil mulls. The samples of polymers P1–P4 were formed as thin films between KBr plates.

The molecular mass distribution of the polymers was determined by gel permeation chromatography (GPC) on a Knauer chromatograph with a Smartline RID 2300 differential refractometer as the detector, with a set of two Phenomenex columns (Phenogel sorbent with a pore size of 10^4 and 10^5 Å; THF as the solvent, 2 mL/min; 40°C). The columns were calibrated against 13 polystyrene standards.

The UV/Vis spectra of iridium-containing complexes and polymers were recorded in CH_2Cl_2 on a Perkin Elmer Lambda 25 spectrometer. The photoluminescence spectra were obtained on a Perkin Elmer LS 55 fluorescence spectrometer. The relative quantum yields were determined at room temperature in degassed CH_2Cl_2 solutions; the excitation wavelength was 370 nm. The quantum yields were calculated relative to Rhodamine 6G in ethanol ($\Phi f = 0.95$) [16] by the procedure described in [17].

Differential scanning calorimetry (DSC) was run on a DSC 204 F1 Phoenix (Netzsch) instrument in a dry argon flow (flow rate of 20 cm^3/min; heating rate of 5°C/min).

The electroluminescence spectra, current–voltage and brightness–voltage characteristics, and CIE chromaticity coordinates were determined on model OLED devices without encapsulation using an automated computer-coupled assembly, including a GW INSTEK PPE-3323 power source, a GW INSTEK GDM-8246 digital multimeter, and an Ocean Optics USB 2000 spectrofluorimeter.

Synthesis of NBEpicIr(Ppy)$_2$ (I). A solution of bicyclo[2.2.1]hept-5-ene-2-carbonyl chloride (0.12 g, 0.766 mmol) in CH_2Cl_2 (5 mL) was added to a solution of (HOpic)Ir(Ppy)$_2$ (0.10 g, 0.157 mmol) and triethylamine (0.16 g, 1.58 mmol) in CH_2Cl_2 (10 mL) and the mixture was stirred at room temperature for 2 h. Water (20 mL) was added, and extraction with chloroform was performed. The extract was dried with magnesium sulfate and the solvent was evaporated in vacuo. Recrystallization of the residue from $CHCl_3$ gave 0.12 g (87%) of product **I** as an air-stable yellow crystalline solid. The compound contained a solvate chloroform molecule.

For $C_{37}H_{29}N_3O_4Cl_3Ir$		
Anal. calcd., %	C, 50.82	H, 3.36
Found, %	C, 50.78	H, 3.39

IR (ν, cm^{-1}): 3054 w, 3033 w, 1101 m, 1062 m, 1030 m, 1012 m, 757 s, 731 s (C_{Ar}–H); 2927 vs, 1379 s, 1334 m, 1317 w, 1163 m (C_{Alk}–H); 1607 m (C···O); 1583 m, 1462 vs, 1265 m (C=C_{Ar}); 494 vw (Ir–O).

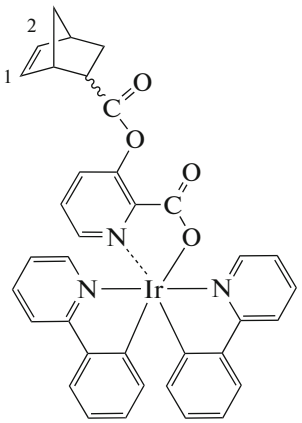

(I)

^{1}H NMR ($CDCl_3$; δ, ppm): 8.79 dd (1H, Pyr, J = 6.4, 0.7 Hz), 7.82–7.89 m (2H, Pic + Pyr), 7.70 t (3H, J = 8.2 Hz, Pic + Pyr), 7.45–7.62 m (4H, Pic + Pyr), 7.3 m (1H, Pyr), 7.15 t (1H, Pyr, J = 7.3 Hz), 6.72–6.98 m (5H, Ph), 6.37 dd (1H, Ph, J = 7.9, 0.9 Hz), 6.22 dd (1H, H^2, J = 5.4, 2.9 Hz), 6.14 d (1H, pyr, J = 7.7 Hz), 6.09 m (1H, H^1), 2.96 br.s (1.8 H, *endo*-NBE), 2.62–2.73 m (0.2 H, *exo*-NBE), 1.95–2.28 m (1 H, NBE), 1.48–.65 m (4H, NBE), 0.85–0.92 m (2H, NBE).

^{13}C NMR ($CDCl_3$; δ, ppm): 177.5, 169.3, 167.7, 160.9, 160.7, 148.9, 148.6, 148.1, 146.0, 139.7, 138.3, 138.1, 137.9, 137.3, 137.2, 137.1, 134.9, 132.5, 132.4, 130.0, 129.8, 129.6, 126.6, 124.3, 122.3, 122.8, 121.2, 119.0, 118.5, 49.9, 46.6, 46.5, 45.7, 42.6, 30.9, 29.7.

NBEpicIr(Dfppy)$_2$ (II) was synthesized similarly to complex **I** from (HOpic)Ir(Dfppy)$_2$ (0.0702 g, 0.098 mmol) and bicyclo[2.2.1]hept-5-ene-2-carbonyl chloride (0.0784 g, 0.501 mmol). The product was recrystallized from CH_2Cl_2 to give 0.0790 g (87.6%) of air-stable yellow crystals.

For $C_{36}H_{24}F_4N_3O_4Ir$		
Anal. calcd., %	C, 52.04	H, 2.92
Found, %	C, 52.10	H, 2.83

IR (KBr; ν, cm^{-1}): 3675 w, 3371 w, 3211 w, 3081 m, 1101 m, 1012 m, 763 m, 722 m (C_{Ar}–H); 2924 vs, 1376 m, 1340 m, 1163 m (C_{Alk}–H); 1604 s (C···O); 1574 s, 1462 s, 1293 m (C=C_{Ar}); 1249 m, 1163 m (C–F); 568 w, 526 w (Ir–O).

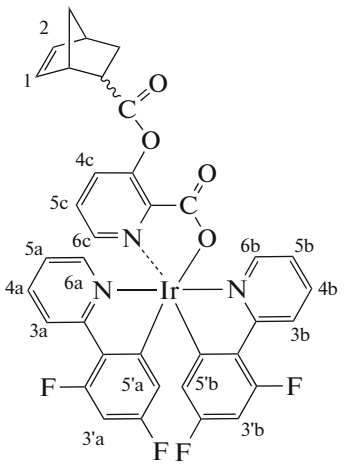

(**II**)

^{1}H NMR ($CDCl_3$; δ, ppm): 8.74 d (1H, H^{6b} Pyr, J = 5.2 Hz,), 8.21–8.31 m (2H, H^{3a}, and H^{3b}), 7.78 t (2H, H^{5c}, and H^{6c} J = 7.76 Hz), 7.34–7.67 m (2H, H^{6a}, and H^{4c}), 7.21–7.23 m (1H, H^{5b}), 6.99–7.01 m (1H, H^{5a}), 6.33–6.53 m (2H, $H^{3'a}$, and $H^{3'b}$), 6.21–6.24 m (1H, H^2), 6.08–6.12 m (1H, H^1), 5.81 dd (1H, $H^{5'b}$, J = 8.5, 2.6 Hz), 5.52 dd (1H, $H^{5'a}$, J = 8.9, 2.3 Hz), 2.69 br.s (1.5 H, *endo*-NBE), 2.61–2.70 m (0.5 H, *exo*-NBE), 2.06–2.14 m (1 H, NBE), 1.26–1.51 m (5H, NBE), 0.83–0.90 m (1H, NBE).

^{13}C NMR ($CDCl_3$; δ, ppm): 177.3, 165.8, 164.4, 160.7, 152.0, 149.7, 148.6, 148.0, 145.9, 139.5, 138.4, 138.1, 135.8, 134.4, 132.5, 130.0, 128.8, 127.3, 123.4, 122.9, 122.6, 114.4, 98.1, 51.7, 49.7, 46.6. 45.6, 44.0, 42.6, 41.9, 29.9

Synthesis of copolymer P1. The third-generation Grubbs catalyst (0.0031 g, 0.0034 mmol) was added to a mixture of monomers **I** (0.0312 g, 0.036 mmol) and L^1 (0.0965 g, 0.353 mmol) in CH_2Cl_2 (5 mL). The mixture was stirred at room temperature. The reaction was monitored by thin layer chromatography. After completion of copolymerization (2 h), several drops of vinyl ethyl ether were added to the reaction mixture, and the mixture was stirred for 30 min. The copolymer was precipitated with hexane, reprecipitated with methanol from CH_2Cl_2, and dried in vacuo to a constant weight. The yield of copolymer P1 was 0.11 g (89%).

For $C_{236}H_{218}N_{13}O_4Ir$		
Anal. calcd., %	C, 81.21	H, 6.27
Found, %	C, 81.15	H, 6.30

IR (ν, cm^{-1}): 3145 w (C=C–H), 3051 m, 1062 m, 1030 m, 1003 m, 748 vs, 722 vs (C_{Ar}–H); 2938 s (C–H), 1381 w, 1154 m (C_{Alk}–H); 1651 m (C=O); 1598 s, 1482 vs, 1461 vs, 1228 m (C=C_{Ar}); 970 m (C–C); 565 w, 529 w (Ir–O).

^{1}H NMR ($CDCl_3$; 200 MHz; δ, ppm): 0.6–4.23 m (97 H), 4.93–5.52 m (20 H), 7.05–7.33 m (76 H, Ar), 7.80–8.06 m (23 H, Ar).

M_n = 34560, M_w/M_n = 1.7; T_g = 179.0°C.

Copolymer P2 was synthesized similarly to P1. The copolymerization time was 4 h. The reaction of monomer **I** (0.0270 g, 0.031 mmol) and monomer L^2 (0.0923 g, 0.321 mmol) gave 0.10 g (87%) of copolymer P2.

For $C_{236}H_{198}N_{13}O_{14}Ir$		
Anal. calcd., %	C, 78.02	H, 5.51
Found, %	C, 78.11	H, 5.60

IR (ν, cm^{-1}): 3125 w (C=C–H), 3060 m, 1101 m, 1062 w, 1035 w, 1 006 vw, 725 vs (C_{Ar}–H); 2947 m (C–H), 1379 s, 1157 vs (C_{Alk}–H); 1690 vs, 1651 m (C=O); 1598 m, 1476 m, 1444 vs, 1278 vs (C=C_{Ar}); 970 w (C–C); 568 w, 524 w (Ir–O).

^{1}H NMR ($CDCl_3$; 200 MHz; δ, ppm): 0.6–3.27 m (77 H), 4.82–5.60 m (22 H), 7.08–8.18 m (99 H, Ar).

M_n = 22200, M_w/M_n = 1.4; T_g = 188°C.

Copolymer P3 was synthesized similarly to P1. The copolymerization time was 2 h. The reaction of monomer **II** (0.0329 g, 0.036 mmol) and monomer L^1 (0.0982 g, 0.347 mmol) gave 0.11 g (85%) of copolymer P3.

IR (ν, cm^{-1}): 3122 vw (C=C–H), 3053 m, 1062 m, 1027 m, 1004 m, 751 vs (C_{Ar}–H); 2944 s (C–H), 1373 m, 1154 s (C_{Alk}–H); 1660 s (C=O); 1598 vs, 1488 vs, 1465 vs, 1231 m (C=C_{Ar}); 1243 m, 1154 s (C–F); 973 w (C–C); 565 w, 526 w (Ir–O).

^{1}H NMR ($CDCl_3$; 200 MHz; δ, ppm): 0.9–4.17 m (97 H), 4.96–5.55 m (22 H), 7.15–7.33 m (74 H, Ar), 7.95–8.14 m (21 H, Ar).

For $C_{236}H_{214}N_{13}O_4F_4Ir$		
Anal. calcd., %	C, 79.51	H, 6.06
Found, %	C, 79.60	H, 6.01

M_n = 59410, M_w/M_n = 1.7; T_g = 188°C.

Copolymer P4 was synthesized similarly to P1. The copolymerization time was 4 h. The reaction of monomer **II** (0.0251 g, 0.026 mmol) and monomer L^2 (0.0770 g, 0.268 mmol) gave 0.90 g (93%) of copolymer P4.

For $C_{236}H_{194}F_4N_{13}O_{14}Ir$		
Anal. calcd., %	C, 76.51	H, 5.29
Found, %	C, 76.63	H, 5.35

IR (ν, cm^{-1}): 3128 w (C=C–H), 3063 m, 1101 w, 1068 w, 1038 m, 754 vs (C_{Ar}–H); 2950 m (C–H), 1379 s, 1168 s (C_{Alk}–H); 1690 vs (C=O); 1559 m, 1488 m, 1479 s

(C=C_{Ar}); 1240 w, 1142 m (C–F); 973 m (C–C); 568 w, 524 w (Ir–O).

^{1}H NMR ($CDCl_3$; 200 MHz; δ, ppm): 0.95–3.54 m (77 H), 4.95–5.52 m (22 H), 7.10–8.18 m (95 H, Ar).

M_n = 29940, M_w/M_n = 1.2; T_g = 194°C.

X-ray diffraction study of **I** was carried out on a Bruker D8 Quest diffractometer (ω-scan mode, MoK_α-radiation, λ = 0.71073 Å). The experimental sets of reflection intensities were integrated using the SAINT program [18]. The structure of complex **I** was solved by direct methods and refined with full-matrix least-squares method on F^2_{hkl}. All non-hydrogen atoms were refined in the anisotropic approximation. The hydrogen atoms were placed into geometrically calculated positions and refined in the riding model. The SHELXTL program package was used for calculations [19]. The absorption corrections were applied using the SADABS program [20]. The crystal of compound **I** was found to contain chloroform solvate molecules in general positions and in 1 : 1 ratio to the iridium complex molecule. The norbornene moieties and one of the $CHCl_3$ solvate molecules are disordered over two positions. The crystallographic data and selected refinement parameters are summarized in Table 1. Selected bond lengths and bond angles are given in Table 2.

The crystallographic data for compound **I** are deposited with the Cambridge Crystallographic Data Centre (CCDC no. 1878882; deposit@ccdc.cam.ac.uk or https://www.ccdc.cam.ac.uk/structures/).

Fabrication of OLED devices. A glass plate with a deposited ITO layer (120 nm, 15 Ω/cm^2) (Lum Tec), acting as an anode, was used as the substrate for OLEDs designed as ITO/Ir-polymer (40 nm)/BATH (30 nm)/Alq_3(30 nm)/Yb (150 nm). The copolymer emission layer was deposited from a CH_2Cl_2 solution of the copolymer (5 mg/mL) on a Spincoat G3-8 centrifuge (3000 rpm, 30 s) and dried in vacuum at 70°C for 3 h. The layer thickness was determined by a META-900 ellipsometer. The hole blocking BATH layer, the electron-transporting Alq_3 BATH, and a Yb layer acting as the cathode were deposited by vacuum evaporation (10^{-6} mm Hg) from separate resistive thermal evaporators. The layer thickness was monitored by a calibrated quartz resonator. The active area of the devices was a circle with a diameter of 5 mm.

RESULTS AND DISCUSSION

Picolinate-anchored norbornene-containing iridium complexes **I** and **II** were prepared as depicted in Scheme 1:

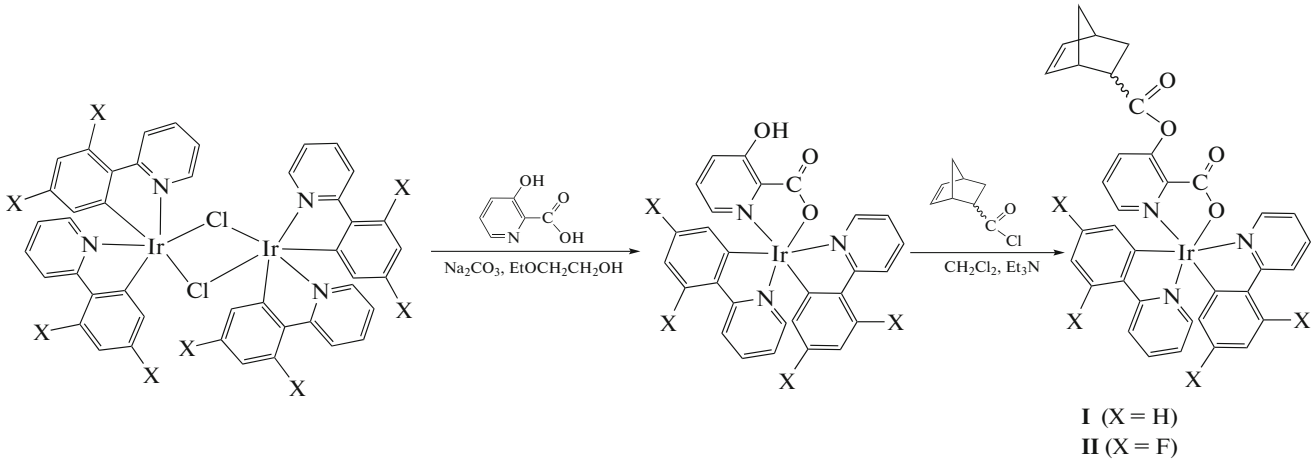

Scheme 1.

Compounds **I** and **II** were isolated in high yields as air-stable yellow crystalline solids soluble in chloroform, CH_2Cl_2, and DME. According to NMR data, the products exist in solutions as 75 : 25 mixtures of *endo* and *exo* isomers.

The structure of complex **I** was determined by X-ray diffraction. The asymmetric part of the unit cell of **I** accommodates two molecules A and B, which are Δ and Λ isomers, respectively (Fig. 1). The Ir(1) central atom has an octahedral environment and coordinates three ligands: two cyclometalated (Ppy) and one additional (NBEpic) ligands. The Ppy ligands are *cis*-C–C- and *trans*-N–N-arranged relative to each other. The angle between the apical nitrogen atoms is 174.54(16)° (A) and 173.93(18)° (B). The deviations of Ir atoms from the base planes of the octahedra in molecules A and B are markedly different: 0.005 and 0.113 Å. The NIr(1)C angles in the Ppy ligands vary in a narrow range of 80.2(2)°–81.1(2)°. The O(1)Ir(1)N(1) chelate angles of the norbornene picolinate groups are considerably smaller: 75.79(15)° (A) and 75.99(16)° (B).

Table 1. Crystallographic data and X-ray diffraction experiment and structure refinement details for complex **I**

Parameter	Value
Formula	$C_{37}H_{29}N_3O_4Cl_3Ir$
M	878.18
System	Triclinic
Space group	$P\bar{1}$
Temperature, K	100(2)
a, Å	14.1292(10)
b, Å	16.2045(11)
c, Å	16.3443(11)
α, deg	76.056(2)
β, deg	65.665(2)
γ, deg	77.927(2)
V, Å^3	3283.5(4)
Z	4
ρ(calcd.), g/cm^3	1.776
μ, mm^{-1}	4.357
F(000)	1728
Crystal size, mm	0.35 × 0.35 × 0.22
Range of θ, deg	2.37–28.00
Reflection indices	$-18 \le h \le 18$, $-21 \le k \le 21$, $-21 \le l \le 21$
Number of collected reflections	38962
Number of unique reflections (R_{int})	15738 (0.0382)
Number of reflections with $I > 2\sigma(I)$	12649
Absorption correction (max/min)	SADABS (0.3969/0.1915)
Data/constraints/parameters	15738/277/872
Goodness of fit (F^2)	1.054
R_1/wR_2 ($I > 2\sigma(I)$)	0.0429/0.1045
R_1/wR_2 (for all reflections)	0.0584/0.1101
$\Delta\rho_{max}/\Delta\rho_{min}$, e Å^{-3}	2.807/–1.264

In each A and B molecule of complex **I**, the norbornene moiety is disordered over two positions with equal occupancies. In molecule A, norbornene is in the *endo* form in both disordered positions, while in molecule B, it is in the *endo* and *exo* forms. Thus, 75% of the iridium complexes in the crystal of **I** contain *endo*-norbornene moiety, while the rest 25% contain *exo*-norbornene moiety, which is in line with the data of NMR spectra.

The molecules of Ir(1A) and Ir(1B) complexes are packed in centrosymmetrical pairs with parallel arrangement of Ppy ligands (Fig. 2a, 2b). In a pair of Ir(1A) complex molecules, the parallel Ppy ligands are overlaid by the N(2A)C(15A–21A) pyridine moieties (Fig. 2c). The centers of the pyridine rings are shifted relative to each other by 0.97 Å. The distance between them (3.54 Å) is close to the distance between the parallel planes of the Ppy ligands (3.38 Å). These geometric characteristics may be indicative of π–π-interaction between the N(2A)C(15A–21A) pyridine moieties [21].

In the second complex Ir(1B), unlike complex Ir(1A), the parallel Ppy ligands of two neighboring molecules are completely shifted relative to each other: the pyridine moiety of a Ppy ligand is inserted into the gap between the phenyl and pyridine moieties of another Ppy ligand (Fig. 2d). The distances between

Table 2. Selected bond lengths (*d*) and bond angles (ω) in complex **I**

Bond	Molecule A	Molecule B	Angle	Molecule A	Molecule B
	d, Å			ω, deg	
Ir(1)–O(1)	2.159(4)	2.147(4)	O(1)Ir(1)C(36)	172.16(17)	172.30(19)
Ir(1)–N(1)	2.129(4)	2.134(5)	N(1)Ir(1)C(25)	173.69(18)	169.83(19)
Ir(1)–N(2)	2.040(4)	2.046(4)	N(2)Ir(1)N(3)	174.54(16)	173.93(18)
Ir(1)–N(3)	2.026(4)	2.026(4)	O(1)Ir(1)N(1)	75.79(15)	75.99(16)
Ir(1)–C(25)	2.000(5)	1.987(5)	N(2)Ir(1)C(25)	80.4(2)	80.2(2)
Ir(1)–C(36)	1.976(5)	1.983(6)	N(3)Ir(1C(36)	80.63(19)	81.1(2)
O(1)–C(1)	1.276(7)	1.254(7)	N(1)Ir(1)C(36)	97.24(18)	99.0(2)
O(2)–C(1)	1.225(6)	1.238(7)	O(1)Ir(1)C(25)	99.38(17)	95.52(18)
C(1)–C(2)	1.524(8)	1.506(8)	C(25)Ir(1)C(36)	87.82(19)	90.0(2)
C(2)–N(1)	1.346(6)	1.351(7)	N(1)Ir(1)N(3)	87.73(16)	91.92(17)
C(2)–C(3)	1.389(8)	1.390(8)	N(1)Ir(1)N(2)	95.36(17)	93.96(18)
C(3)–O(3)	1.376(7)	1.374(7)	N(3)Ir(1)C(25)	96.84(19)	94.18(19)
O(3)–C(7)	1.367(8)	1.379(8)	O(1)Ir(1)N(3)	95.33(15)	93.16(16)
C(7)–O(4)	1.193(8)	1.180(8)	O(1)Ir(1)N(2)	89.79(15)	89.75(16)
N(2)–C(19)	1.357(7)	1.354(7)	N(2)Ir(1)C(36)	94.50(19)	96.5(2)
C(19)–C(20)	1.441(8)	1.445(8)			
C(20)–C(25)	1.419(7)	1.405(7)			
N(3)–C(30)	1.350(6)	1.367(6)			
C(30)–C(31)	1.461(7)	1.453(7)			
C(31)–C(36)	1.412(7)	1.429(8)			

the centers of the neighboring Ph···Py and Py···Py moieties are 4.05 and 4.44 Å, respectively, which is much greater than the interplanar distance between parallel Ppy ligands (3.44 Å). Apparently, there is no π–π interactions between two Ir(1B) complex molecules.

Carbazole-based polymers are known to have optimal energy levels for Ir complexes with cyclometalated Dfppy ligands [7]. The carbazole groups in polymeric emitters also improve their charge transport and electroluminescent characteristics [22, 23]. Therefore, for

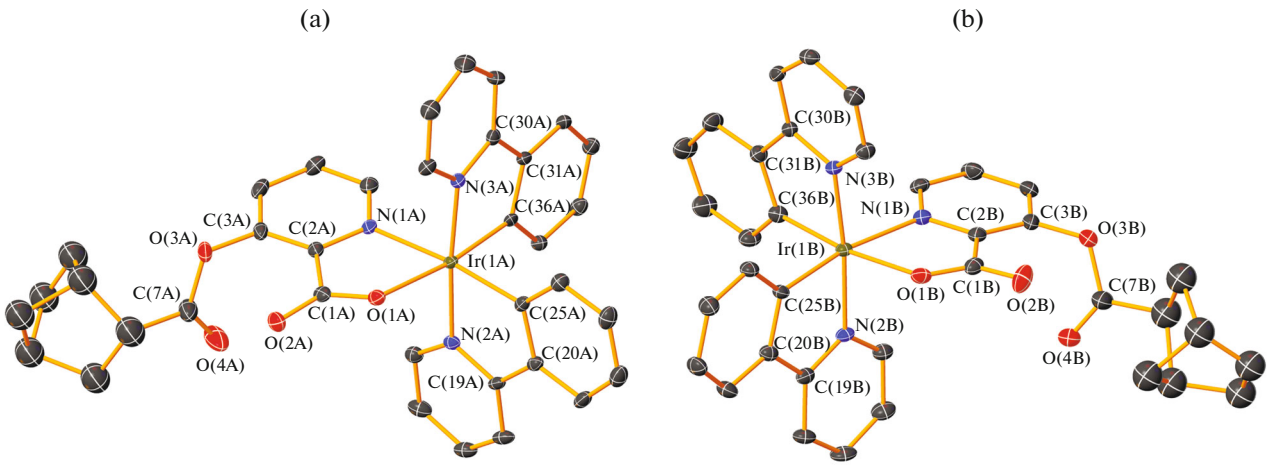

Fig. 1. Molecular structures of (a) Δ and (b) Λ isomers of complex **I**. The thermal ellipsoids are drawn at 30% probability level. The hydrogen atoms and $CHCl_3$ solvate molecules are omitted for clarity.

the ROMP preparation of iridium-containing copolymers, we used norbornene comonomers with carbazole groups. Copolymerization proceeded in the presence of third-generation Grubbs catalyst at room temperature and afforded iridium-containing copolymers P1–P4 (Scheme 2).

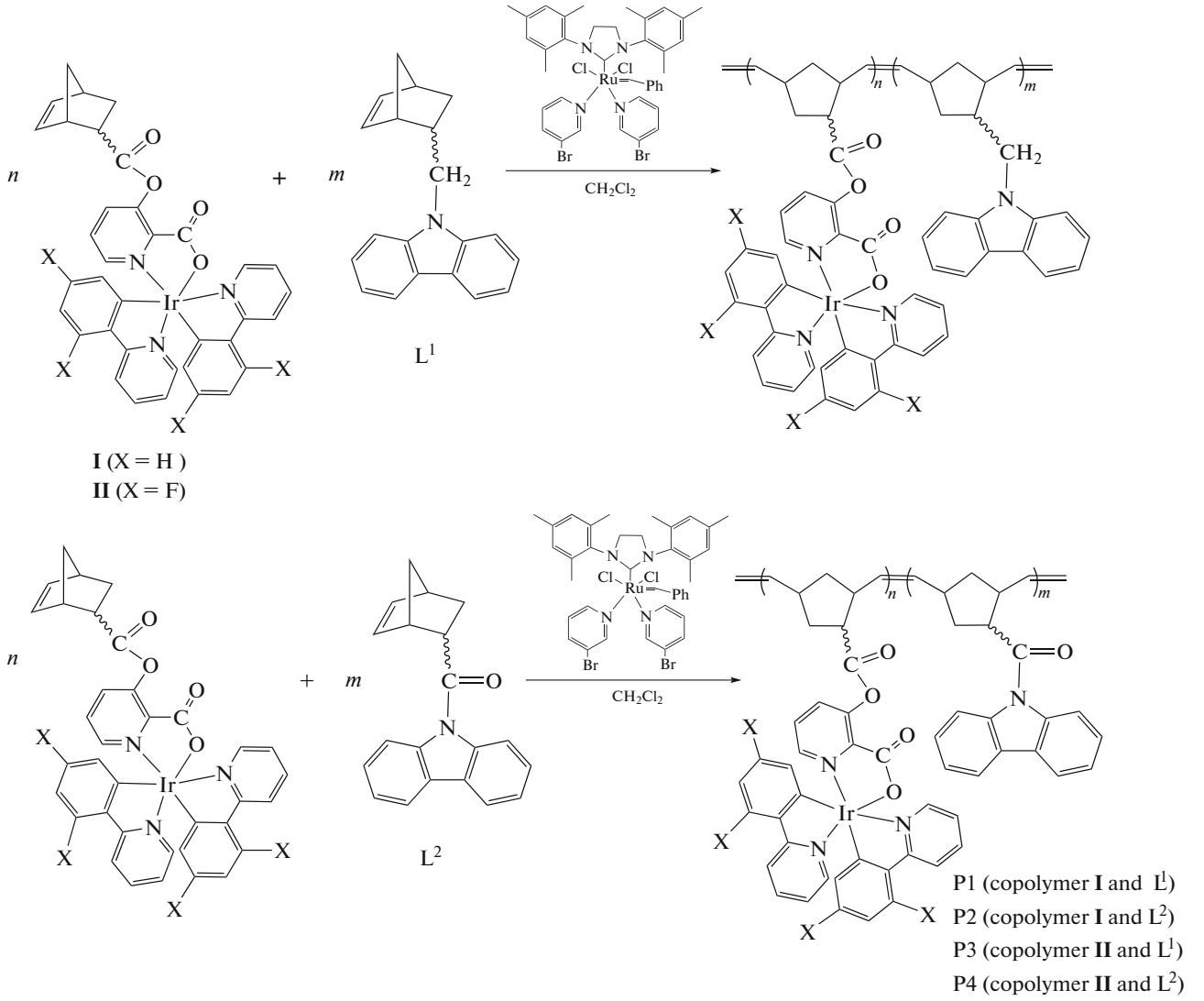

The initial ratio of the iridium- and carbazole-containing comonomers *n* : *m* was 1 : 10 in all cases. The Grubbs catalyst was used in 1 mol % amount with respect to the total amount of comonomers taken for the reaction. According to thin layer chromatography data, copolymerizations were completed in 2–4 h. The copolymers P1–P4 were isolated as air-stable yellow powders readily soluble in THF, CH_2Cl_2, and $CHCl_3$. The composition of copolymers was confirmed by elemental analysis and ^{1}H NMR spectroscopy.

The UV/Vis spectra of complexes **I** and **II** (Fig. 3, Table 3) resemble the spectra of known iridium(III) picolinate complexes (Pic)Ir(Ppy)$_2$, (Pic)Ir(Dfppy)$_2$ (PicH = picolinic acid), (HOPic)Ir(Ppy)$_2$, and (HOPic)Ir(Dfppy)$_2$ [24–26].

The UV/Vis spectra of complexes **I** and **II** are similar and contain intense bands with peaks at 261 nm (**I**) and 253 nm (**II**), corresponding to ligand-centered (LC) singlet $^1(\pi-\pi^*)$ transitions in the aromatic cyclometalated Ppy and Dfppy ligands, respectively [27]. Weak absorption bands in the 350–400 nm ($\varepsilon < 6000$) can be assigned to spin-allowed metal to ligand charge transfer (^{1}MLCT) singlet transitions. The bands in the 430–500 nm range ($\varepsilon < 2500$) are due to spin-forbidden ^{3}LC/^{3}MLCT transitions [25–27]. The absorption spectra of copolymers P1–P4 (Fig. 3, Table 3) exhibit, apart from the bands typical of complexes **I** and **II**, also additional intense bands at 250–340 nm caused by $^1(\pi-\pi^*)$ transitions in the carbazole moieties.

The PL spectra of complexes **I** and **II** (Fig. 4, Table 3) in CH_2Cl_2 contain bands with peaks at about 460–500 nm

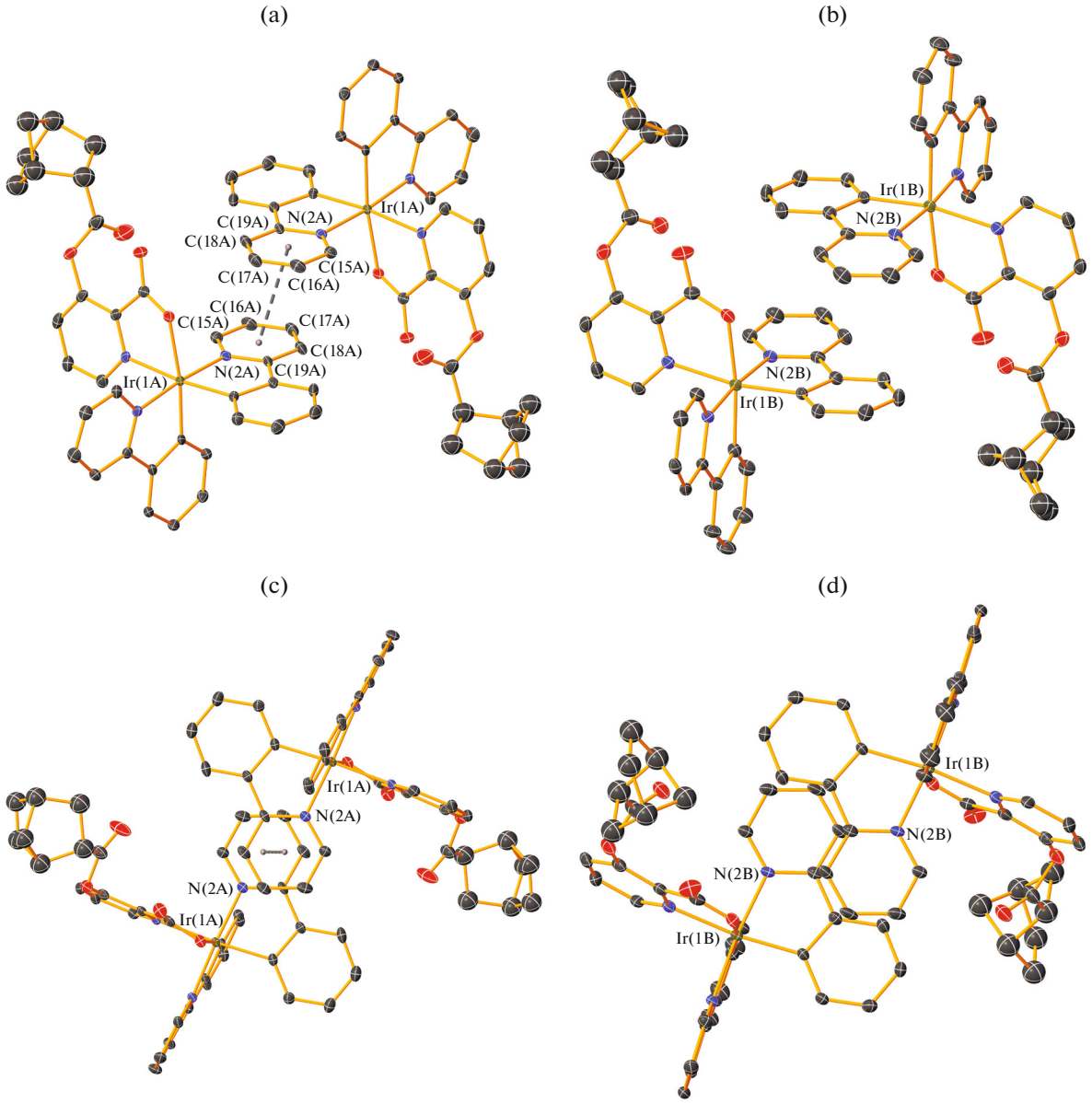

Fig. 2. Fragments of crystal packings of molecules (a, c) A and (b, d) B of complex **I**. The thermal ellipsoids are drawn at 30% probability level. The hydrogen atoms and $CHCl_3$ solvate molecules are omitted for clarity.

corresponding to mixed LC/MLCT transitions in the cyclometalated iridium complexes [25–27]. Unlike vibronically structured PL spectrum of complex **II**, the spectrum of complex **I** is broad and non-structured, which is probably due to predominance of MLCT transitions [28]. The relative quantum yield of fluorinated complex **II** (65.8%) is much higher than that of non-fluorinated complex **I** (2.3%). A similar behavior was noted previously for pairs of complexes $(HOPic)Ir(Dfppy)_2$/$(HOPic)Ir(Ppy)_2$ and $(MePic)Ir(Dfppy)_2$/$(MePic)Ir(Ppy)_2$, with the relative PL quantum yields of 94/20% and 72/15%, respectively [26]. The authors ascertained that the rates of non-radiative deactivation of fluorinated iridium complexes are markedly lower than the rates of analogous processes of their non-fluorinated analogues. Apparently, the difference between the relative quantum yields of complexes **I** and **II** is due to the same factors.

The PL spectra of complexes **I** and **II** in the crystalline state (Fig. 4) show aggregative emission as broad non-structured bands [29]. The red shift (~35 nm) of the emission band of complex **I** is caused by the detected intermolecular π–π interactions in the crystal.

Along with the broad bands for cyclometalated iridium complexes (480–521 nm), the PL spectra of copolymers P1, P2, and P4 in CH_2Cl_2 (Fig. 5a, Table 3) exhibit bands in the 416–433 nm range corresponding to the excimer emission of carbazole groups [30, 31].

The absence of emission bands for the polymer matrix in the spectrum of P3 attests to more efficient excitation energy transfer from the carbazole groups to iridium-containing groups by the Förster mechanism [32] and results in increasing relative quantum yield of P3 in comparison with other copolymers. The PL spectra of copolymers P1–P4 as thin films (Fig. 5b, Table 3) exhibit only emission bands of metal-containing groups, while virtually no emission of the polymer matrix is observed.

The electroluminescent properties of copolymers P1–P4 were studied using model OLEDs designed as ITO/Ir-copolymer (40 nm)/BATH (30 nm)/Alq_3 (30 nm)/Yb. The EL spectra of polymers P1–P4 and the operating characteristics of OLEDs based on them are shown in Figs. 6, 7 and in Table 4.

The EL spectra of copolymers P1–P4 contain bands with peaks at 500–530 nm corresponding to the ^{3}LC/^{3}MLCT transitions in the cyclometalated iridium complexes attached to the polymer chain. The absence of emission from carbazole groups indicates the efficient Förster excitation energy transfer from the polymer matrix to iridium-containing groups [32]. The CIE (Commision Internationale del'Eclairage) chromaticity coordinates for the emission of light emitting diodes (Table 4) correspond to yellow-green (P1, P2), green (P3), and blue-green (P4) colors and virtually does not change over the whole range of voltages. The highest EL characteristics were found for light emitting diodes based on copolymers P3 and P4 (Table 4).

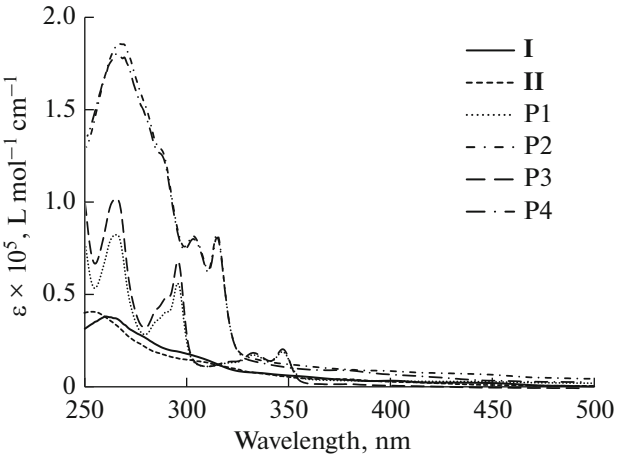

Fig. 3. Absorption spectra of complexes **I** and **II** and copolymers P1–P4 in a CH_2Cl_2 solution.

Thus, new cyclometalated iridium(III) complexes with a norbornene-substituted picolinate ligand were synthesized and converted via ROMP to new carbochain copolymers P1–P4 with side-chain carbazole

Table 3. Photophysical characteristics of complex **I** and **II** and polymers P1–P4

Compound	λ_{abs} (nm)/logε	λ_{em} (nm)		Quantum yield, %
		film	CH_2Cl_2	CH_2Cl_2
I	261 (4.57), 293 sh (4.29), 330 sh (3.90), 355 sh (3.76), 400 (3.51), 430 sh (3.35), 430 sh (3.24), 481 sh (2.71)	538 (in the crystal)	503	2.3
II	253 (4.61), 284 sh (4.29), 330 sh (3.91), 354 sh (3.71), 395 (3.51), 435 sh (3.22), 481 sh (2.71)	501 (in the crystal)	467, 497	65.8
P1	264 (4.90), 285 sh (4.52), 290 sh (4.58), 295 (4.72), 322 sh (4.03), 332 (4.17), 347 (4.21), 367 sh (3.22), 383 sh (3.13), 395 sh (3.12), 440 sh (3.01), 480 sh (2.64)	441 sh, 518	416, 440, 524, 550 sh	12.5
P2	266 (5.26), 278 sh (5.18), 303 (4.87), 315 (4.89), 333 sh (4.05), 360 sh (3.87), 380 sh (3.77), 410 sh (3.67)	521	421, 433, 505 sh, 521	15.3
P3	265 (5.01), 286 sh (4.63), 290 (4.67), 295 (4.83), 322 sh (4.14), 333 (4.27), 347 sh (4.31), 382 sh (3.21), 410 sh (3.06), 455 sh (2.86)	482 sh, 498	468, 504	70.0
P4	265 (5.24), 268 sh (5.23), 277 sh (5.17), 285 sh (5.09), 303 (4.88), 315 (4.89), 333 sh (4.01), 360 sh (3.80), 380 sh (3.78), 410 sh (3.52)	480 sh, 499	428 sh, 468, 505	6.5

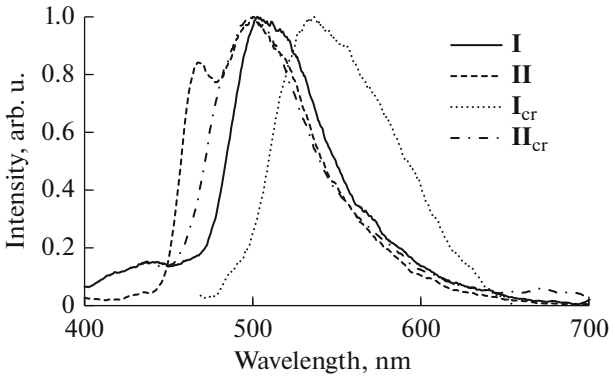

Fig. 4. PL spectra of complexes **I** and **II** at room temperature: (**I**, **II**) in solution and (**I_{cr}**, **II_{cr}**) in the crystalline state, λ_{ex} = 370 nm.

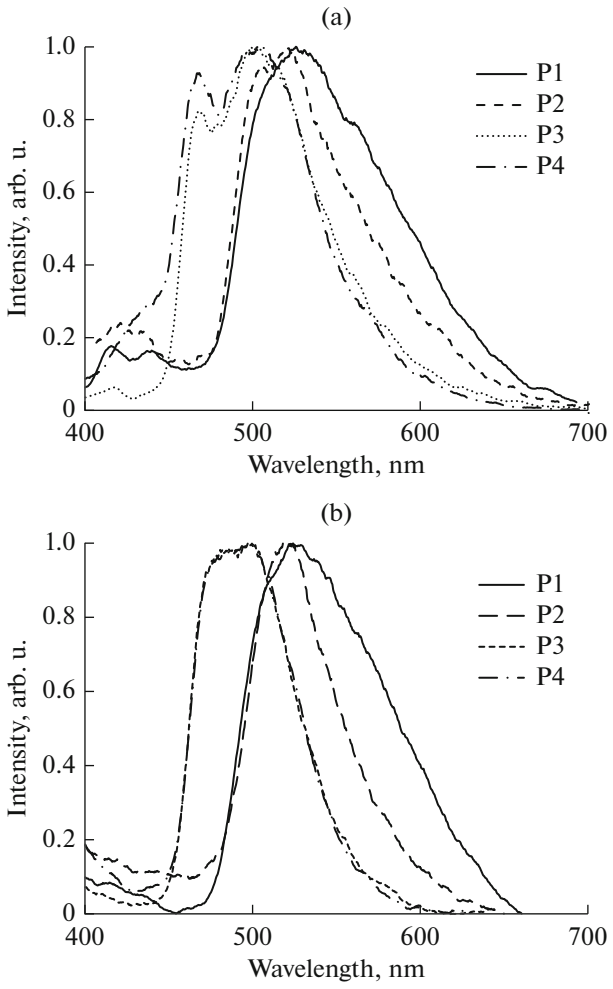

Fig. 5. PL spectra of copolymers P1–P4 (a) in a CH_2Cl_2 solution at room temperature and (b) in thin film, λ_{excit} = 370 nm.

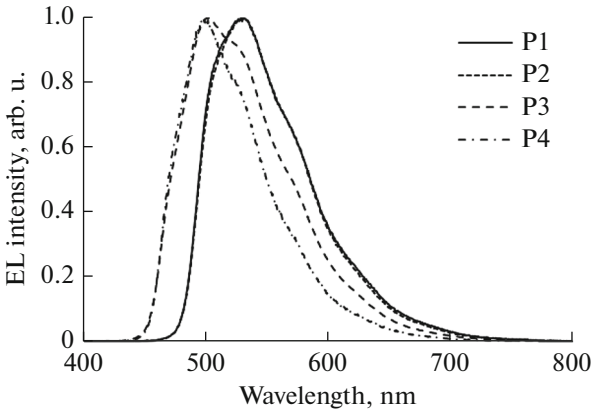

Fig. 6. Normalized EL spectra of copolymers P1–P4.

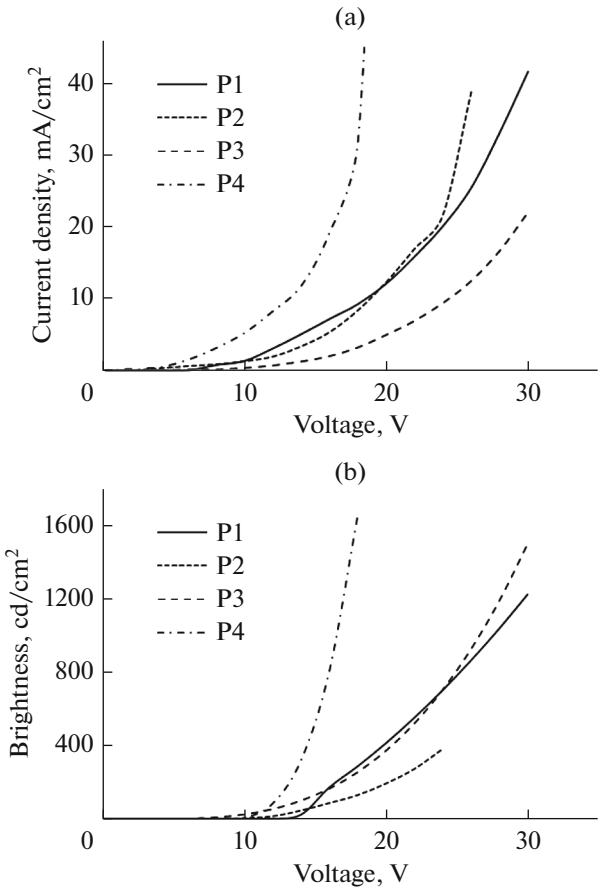

Fig. 7. (a) Current–voltage and (b) brightness–voltage characteristics of light-emitting diodes based on polymers P1–P4.

and iridium-containing moieties. The resulting polymeric emitters show intense yellow-green, green, and blue-green PL and EL. The maximum EL brightness, current efficiency, and power efficiency were attained with emitters P3 and P4.

Table 4. Performance characteristics of light-emitting diodes based on polymers P1–P4

Ir-polymer	λ_{max}, nm	Turn-on voltage, V*	Maximum brightness, cd/m^2 **	Maximum current efficiency, cd/A**	Maximum power efficiency, lm/W**	Chromaticity coordinates in the CIE diagram
P1	529, 555 sh	12	1220 (30 V)	3.42 (18 V)	0.60 (18 V)	$x = 0.32$ $y = 0.62$
P2	530, 556 sh	8	380 (24 V)	1.60 (16 V)	0.31 (16 V)	$x = 0.31$ $y = 0.62$
P3	503, 514 sh, 555 sh	6	1493 (30 V)	8.04 (16 V)	1.88 (12 V)	$x = 0.22$ $y = 0.45$
P4	501, 516 sh, 556 sh	10	1653 (18 V)	2.69 (14 V)	0.60 (14 V)	$x = 0.18$ $y = 0.42$

* Brightness at 1 cd/m^2.
** The value in parentheses is the voltage at which the performance characteristics were determined.

ACKNOWLEDGMENTS

X-ray diffraction studies were carried out using the research equipment of the Center for Collective Use "Analytical Center of the Institute of Organometallic Chemistry, Russian Academy of Sciences."

FUNDING

This work was performed within the State Assignment (subject no. 44.2, reg. no. AAAA-A16-116122110053-1).

CONFLICT OF INTEREST

The authors declare that they have no conflicts of interest.

REFERENCES

1. *Highly Efficient OLEDs with Phosphorescent Materials*, Yersin, H., Ed., Weinheim: Wiley-VCH, 2008, p. 438.
2. Ulbricht, C., Beyer, B., Friebe, C., Winter, A., et al., *Adv. Mater.*, 2009, vol. 21, p. 4418.
3. *Iridium(III) in Optoelectronic and Photonics Applications*, Zysman-Colman, E., Ed., Chichester: Wiley-VCH, 2017, p. 736.
4. Yusoff, A.R.B.M., Huckaba, A.J., and Nazeeruddin, M.K., *Top Curr. Chem. (Z)*, 2017, vol. 375, p. 39.
5. Lee, S.Yu., Lee, S.E., Oh, Y.N., et al., *J. Nanosci. Nanotechnol.*, 2017, vol. 17, p. 5673.
6. *Nanomaterials, Polymers and Devices: Materials Functionalization and Device Fabrication*, Kong E.S.W., Ed., New Jersey: Wiley-VCH, 2015, p. 195.
7. Xua, F., Kima, H.U., Kima, J.-H., et al., *Prog. Polym. Sci.*, 2015, vol. 47, p. 92.
8. Jayabharathi, J., Jayamoorthy, K., and Thanikachalam, V., *J. Organomet. Chem.*, 2014, vol. 761, p. 74.
9. Liu, S.-J., Wang, P., Zhao, Q., et al., *Adv. Mater.*, 2012, vol. 24, p. 2901.
10. Liu, S., Qiao, W., Cao, G., et al., *Macromol. Rapid Commun.*, 2013, vol. 34, p. 81.
11. Nonoyama, M., *Bull. Chem. Soc. Jpn.*, 1974, vol. 47, p. 767.
12. Kwon, T.-H., Kim, M.K., Kwon, J., et al., *Chem. Mater.*, 2007, vol. 19, p. 3673.
13. Liaw, D.J. and Tsai, C.H., *Polymer*, 2000, vol. 41, p. 2773.
14. Rozhkov, A.V., Bochkarev, L.N., Basova, G.V., et al., *Russ. J. Gen. Chem.*, 2012, vol. 82, no. 12, p. 1895.
15. Love, J.A., Morgan, J.P., Trnka, T.M., et al., *Angew. Chem., Int. Ed. Engl.*, 2002, vol. 41, p. 4035.
16. Magde, D., Wong, R., and Seybold, P.G., *Photochem. Photobiol.*, 2002, vol. 75, p. 327.
17. Demas, J.N. and Crosby, G.A., *J. Phys. Chem.*, 1971, vol. 75, p. 991.
18. *SAINT. Data Reduction and Correction Program. Version 8.34A*, Madison (WI, USA): Bruker AXS, 2014.
19. Sheldrick, G.M., *SHELXTL. Version 6.14. Structure Determination Software Suite*, Madison: Bruker AXS, 2003.
20. Sheldrick, G.M., *SADABS. Version 2014/5. Bruker/Siemens Area Detector Absorption Correction Program*, Madison: Bruker AXS, 2014.
21. Janiak, C., *Dalton Trans.*, 2000, p. 3885.
22. Grimsdale, A.C., Chan, K.L., Martin, R.E., et al., *Chem. Rev.*, 2009, vol. 109, p. 897.
23. Bochkarev, M.N., Vitukhnovskii, A.G., and Katkova, M.A., *Organicheskie svetoizluchayushchie diody (OLED)* (Organic Light-Emitting Diodes (OLEDs)), Nizhny Novgorod: Dekom, 2011.
24. Baranoff, E. and Curchod, B.F.E., *Dalton Trans.*, 2015, vol. 44, p. 8318.
25. You, Y., Kim, K.S., Ahn, T.K., et al., *J. Phys. Chem. C*, 2007, vol. 111, p. 4052.
26. Yi, S., Kim, J.-H., Cho, Y.-J., et al., *Inorg. Chem.*, 2016, vol. 55, p. 3324.
27. Lamansky, S., Djurovich, P., Murphy, D., et al., *Inorg. Chem.*, 2001, vol. 40, p. 1704.
28. Zhao, Q., Liu, S.J., Shi, M., et al., *Inorg. Chem.*, 2006, vol. 45, p. 6152.
29. Hao, Z., Jiang, H., Liu, Y., et al., *Tetrahedron*, 2016, vol. 72, p. 8542.
30. Johnson, G.E., *J. Chem. Phys.*, 1975, vol. 62, p. 4697.
31. Vekikouas, G.E. and Powell, R.C., *Chem. Phys. Lett.*, 1975, vol. 34, p. 601.
32. Förster, T., *Disc. Faraday Soc.*, 1959, vol. 27, p. 7.

Translated by Z. Svitanko